Analyst

Accepted Manuscript

ROYAL SOCIETY OF CHEMISTRY

www.rsc.org/analyst

Analyst

RSCPublishing

ARTICLE

In vitro HER2 protein-induced affinity dissociation of carbon nanotube-wrapped anti-HER2 aptamers for HER2 protein detection†

Javed H. Niazi,[a,*] Sandeep K. Verma,[a] Sarfaraj Niazi[b] and Anjum Qureshi[a]

Cite this: DOI: 10.1039/x0xx00000x

Received 00th January 2012,
Accepted 00th January 2012

DOI: 10.1039/x0xx00000x

www.rsc.org/

A new in vitro assay was developed to detect human epidermal growth factor receptor 2 (HER2) protein based on affinity dissociation of carbon nanotube (CNT)-wrapped anit-HER2 ssDNA aptamers. First, we selected an anti-HER2 ssDNA aptamer (H2) using an in vitro Serial Evolution of Ligands by EXponential enrichment (SELEX) process. Then the fluorescently labelled H2 ssDNAs were tightly packed on CNTs that were previously coupled with magnetic-microbeads (MBs) forming MB-CNT-H2 hybrids. Loading capacity of these MB-CNTs heterostructures (2.8×10^8) was determined to be 0.025 to 3.125 μM of H2. HER2 protein-induced H2 dissociation occurred from MB-CNT-H2 hybrids which was specifically induced by the target HER2 protein with a dissociation constant (K_d) of 270 nM. Stoichiometric affinity dissociation ratio with respect to H2-to-HER2 protein showed approx. 1:1. Our results demonstrated that the developed assay can be an effective approach in detecting the native forms of disease biomarkers in free solutions or biological samples for accurate diagnosis.

1. Introduction

Nanomaterials have gained wide spectrum of applications in biomedical field. They have been effectively utilized to deliver biologically active cargo into the sites of interest for the purposes of cancer diagnosis and therapy.[1-3] Various nanostructured materials such as carbon nanotubes (CNTs),[4] polymeric nanoconjugates,[5, 6] nanoparticles[7, 8] have been explored especially in the cancer therapy.[9] The unique physicochemical properties of CNTs has been exploited as a popular tool in cancer diagnosis and therapy.[10] They are considered one of the most promising nanomaterials with the capability of both detecting the cancerous cells and delivering small therapeutic molecules.[10] In addition, CNTs can effectively shuttle various bio-molecules into cells including drugs,[3, 11] peptides[12] proteins,[13] plasmid DNA,[14] small interfering RNA[15] and aptamers[16] via endocytosis.[17] It is imperative to develop new methods utilizing unique physicochemical properties of CNTs in biomedical applications including detection of cancer biomarkers at their early stage with high specificity and selectivity.

Tumor-targeted therapies require ligands that can bind to cancer cells where aptamers can represent an alternative therapeutic modality. These molecules are small, single-stranded DNA or RNA in nature.[18] Aptamers have broad prospect in therapeutic applications, especially in the cancer field, for example, AS1411, a nucleolin-specific truncated version of an aptamer called GRO29A is currently in advanced clinical trials.[19] Other therapeutic aptamers have been tested for antiviral, anticoagulation, anti-inflammatory, or antiangiogenic properties are already in clinical trials.[20] Macugen is the first clinically approved aptamer made of ssRNA molecule which effectively inhibits macular degeneration.[21] With the aim of creating a more effective tool for the diagnosis of cancer, we considered human epidermal growth factor receptor 2 (HER2) as a target cancer marker protein.

HER2, also known as ErbB2, Neu, CD340 or P185 is a transmembrane tyrosine kinase receptor and a member of the epidermal growth factor receptor (EGFR or ErbB) family. Overexpression of ~20-30% HER2 shown to be associated with aggressive breast cancer cases.[22] The overexpression of HER2 levels is also linked to other cancers including ovarian, lung, gastric, and oral cancers.[22, 23] Therefore, it is imperative to monitor HER2 levels which enables early cancer diagnosis. Existing methods for detecting HER2 are based on expensive biopsies followed by conducting immunohistochemistry (IHC) and fluorescence in situ hybridization (FISH) techniques for detecting HER2 protein levels [24,25]. Synthetic tyrosine kinase inhibitors such as Erlotinib and Gefitinib as well as monoclonal antibodies, such as Cetuximab and Trastuzumab have been developed to inhibit pathological signaling or to recruiting the immune system to cancer cells.[26, 27]

Targeting the HER2 with low molecular weight kinase inhibitors has established this family of receptors as an effective target for novel drugs. Thus, therapeutic use of anti-HER2 aptamers is a promising alternative to the monoclonal antibodies and kinase inhibitors for clinical applications mainly because of their relatively low production cost as well as low batch-to-batch variability.[27] Anti-HER2 aptamers have been increasingly developed that have high affinity and specificity to HER2 which is shown to inhibit proliferation of cultured cancer cells.[28-32] Nevertheless, there is still a need for developing new aptamer variants against cancer biomarkers that potentially serve as inhibitory agents for cancer

diseases. Determination of increase in HER2 protein levels in human serum is an alternative approach of utilizing such aptamers in combination with CNT structures to enable treating the cancer in early stages and effectively preventing traumatic events.

In this paper, we first hypothesized an in-vitro delivery system which utilizes CNTs that carry anti-HER2 aptamers and release specifically when the target HER2 protein is supplied in the synthetic medium. This hypothesis was experimentally tested by first selecting a specific anti-HER2 aptamer using SELEX process. The selected anti-HER2 aptamer was packed around CNTs by physical wrapping that were in turn being previously coupled with MBs. These heterogeneous structures were employed to demonstrate the specific dissociation of anti-HER2 aptamers, which was induced by its strong affinity toward HER2 protein. This feature is most desirable for a ligand molecule to qualify for potential targeted drug-delivery application under in vivo conditions.

2. Experimental

2.1. In vitro selection of ssDNA aptamers that bind HER2

2.1.1. Preparation of HER2 protein coated magnetic beads

Pure and carrier free recombinant HER2 (ErbB2) protein (R&D Systems®) was first conjugated with surface activated magnetic Dynabeads® M-270 Carboxylic Acid (Invitrogen, USA) using carbodiimide coupling method as described by the manufacturer. The HER2 protein coated beads were magnetically separated and washed thrice with 100 µL of PBS, pH 8 containing 0.05% tween 80 and finally resuspended in 100 µL of PBS, pH 7.4 containing 0.1% BSA and stored at 4 °C. Thus obtained HER2 protein coated beads were utilized for in vitro selection of ssDNA aptamers using SELEX process.

2.1.2. Negative selection

Negative selection was carried out as a pre-requisite step to eliminate the non-specific oligos from the initial random ssDNA pool prior to beginning the anti-HER2 aptamer selection process. For this, ~10^{15} diverse ssDNAs molecules (random library) with a following sequence: 5'-GGGCCGTTCGAACACGAGCATG(N)$_{40}$GGACAGTACTCAGGTCATCCTAGG-3' (pool-1) was incubated with each aliquot of ~2×10^7 beads coated with (i) ethanolamine, (ii) BSA followed by (iii) naked beads to eliminate the non-binders from the main ssDNA pool. The residual ssDNA pool (pool-2) was resuspended in 1:10 diluted human serum (male; blood type, AB+; PANTM Biotech GmbH) in 1X binding buffer (100 mM NaCl, 20 mM Tris–HCl pH 7.6, 2 mM MgCl2, 5 mM KCl, 1 mM CaCl2, 0.02% Tween 20) allowing removal of undesirable oligos, and this mixture containing random free ssDNA pool (pool 3) was finally utilized for SELEX process.

2.1.3. SELEX

It was essential to subject the random ssDNA pool to thermal treatment in order to attain their most stable confirmations before allowing these molecules to be incubated with target protein. Therefore, at the beginning of each selection round, the initial ssDNAs were denatured at 90 °C for 10 min and quickly cooled at 4 °C for 15 min followed by incubation for 7 min at room temperature (25 °C). Pre-treated ssDNA pool was later utilized for the selection of anti-HER2 aptamers using SELEX as per the method described previously.[33] Details of steps involved in SELEX process is schematically shown in Supporting Information (SI) Fig. S1.

The HER2 protein bound sequences were eluted, purified and amplified by symmetric/asymmetric PCR using the following forward primer: 5'-fluorescein-GGGCCGTTCGAACACGAGCATG-3' (F1) and reverse primer: 5'-GGACAGTACTCAGGTCATCCTAGG-3' (R1). Amplified PCR product (dsDNA) carrying the aptamer sequence was labelled fluorescently during the PCR reaction which was extracted after resolving on 2% agarose gel followed by purification using gel extraction kit (QIAquick, Qiagen). Purified dsDNA was further resolved on denaturation polyacrylamide gel electrophoresis (PAGE, 12%) using 7 M urea containing 20% formamide and isolated the target fluorescent ssDNAs by gel excision followed by extraction using a PAGE gel extraction kit (Qiaex II). Thus obtained ssDNAs were measured by a Nanodrop spectrophtometer (Thermo Scientific) and applied the isolated ssDNA fraction in the next selection round as starting pool. The above process was repeated for at least 12 cycles of selection each comprised a series of steps as illustrated in Fig. S1. An optimized PCR program used to amplify the HER2 bound ssDNAs was as follows: initial 15 min denaturation at 95 °C, 35~40 cycles of 30 s denaturation at 94 °C, 30 s annealing at 53 °C and 30 s amplification at 72 °C, respectively with a final extension step at 72 °C for 10 min. The final pool of selected aptamers was cloned using a TOPO-TA cloning kit (Invitrogen) and sequenced. The secondary structure prediction of the aptamer sequences were evaluated using m-fold webserver (utilizes free energy minimizing algorithm) available at http://www.bioinfo.rpi.edu/applications/mfold.[34] As a result, 7 positive clones designated as H1~H7 were obtained, out of which one of the aptamers, H2 was selected for further studies. All the experimental methods related to cloning and screening of positive clones is described in SI section.

2.2. In vitro assay for the affinity displacement/dissociation of anti-HER2 aptamers

2.2.1. Fabrication of MB-CNTs heterostructures and binding assays

Magnetic microbeads (Dynabeads®, M270 Amine, MBs) were covalently coupled with carboxyl-functionalized multi-walled CNTs O.D. × L = 10~20 nm × 5~30 µm (Arry®, Hongkong). Stock CNTs (1 mg/mL) were dispersed in 0.1% tween-20 and the suspension was homogenized by ultrasonication using a probe sonicator (Bandelin, Germany) and a well-dispersed and homogeneous CNT suspension was added with magnetic beads with intermitted agitation to allow physical interaction of CNTs with magnetic beads according to the method previously described [35]. Thus formed uniform layer of CNTs coated magnetic microbeads were isolated by applying an external magnetic field. The magnetic nature of MBs allowed extensive washing of MB-CNTs for the effective removal of unattached CNTs and minimized the surfactant effect. After extensive washing, the inherent brown color of MBs turned black indicating the strong attachment of CNTs on the surface [35]. SEM images were taken for the beads for further confirmation of homogeneous CNT layer coating. To prevent the attachment of surface CNTs present on MB-CNTs, these were suspended in a mild surfactant solution (0.01% tween-20), which facilitated homogenous suspension of MB-CNTs. Thus formed MB-CNTs heterostructures were utilized for further studies.

2.2.2. Physical adsorption of anti-HER2 ssDNAs on MB-CNTs heterostructures

A constant amount (2.8×10^8) of MB-CNTs heterostructures were incubated against varying ssDNA concentrations in 1X binding buffer (BB). Here, the ssDNAs used were 5' labelled with fluorescein in order to trace the fluorescence levels (emission at 523

nm) in the reaction mixture after an excitation at 470 nm. The reaction mixture was incubated on a vortex mixer for 15 min at room temperature. Binding capacity of MB-CNTs with ssDNAs was estimated by measuring the fluorescence (λ_{523}) in the supernatant solution using Nanodrop Fluorspectrometer (Nanodrop Technologies, Inc., USA). The MB-CNT-ssDNA hybrids were washed in a series of steps until the supernatant showed no detectable fluorescence and finally stored at 4 °C until use. The physical wrapping of ssDNAs around CNTs was confirmed by Fourier transform infrared spectroscopy (FTIR; Nicolet 6700). The ssDNA loading capacity of MB-CNTs heterostructures was calculated to be a maximum of 3.125 µM ssDNA with 2.8×10^8 MB-CNTs. Stability tests of MB-CNT-ssDNA hybrid structure were carried out and the detailed steps were described in SI section.

2.2.3. HER2 protein dependent affinity dissociation of anti-HER2 aptamers from MB-CNT-ssDNA hybrid structures

Ten identical aliquots each carrying 4×10^7 MB-CNT-ssDNA hybrid structures were suspended in 200 µL 1X BB. These aliquots were divided in two pools each with 5 aliquots for test and control groups. A constant 10 µL of 300 nM of HER2 protein prepared from stock 7.5 µg/200 µL in 1X BB and incubated for binding against a series of different concentrations of ssDNA wrapped on MB-CNTs (MB-CNT-ssDNA hybrids). Binding kinetics and HER2 protein induced ssDNA dissociation by unwinding from hybrid structures (affinity separation) was studied. The beads were magnetically separated and the fluorescence was measured in the supernatant which corresponded to the amount of ssDNAs dissociated from MB-CNT-ssDNA hybrids. For controls, instead of HER2 protein, BSA was used as a non-specific protein. The above process was repeated until reaching to a saturation point.

2.2.4. Kinetics of anti-HER2 aptamer (MB-CNT-ssDNAs hybrids) interaction with HER2 protein and dissociation constant (K_d)

First, a standard plot of known concentrations of fluorescein labelled H2 ssDNA versus fluorescence emission at 523 nm was established. A series of controlled number of MB-CNT-ssDNA heterostructures corresponding to 0.025~3.125 µM H2 ssDNAs were incubated with a constant 300 nM HER2 protein in 1X BB solution for 15 min. For respective controls, BSA was used as a non-specific protein. Relative fluorescence units (RFU) directly obtained by fluorospectrometer (which according to the manufacturer, it is derived from the relationship between 2-4 wavelengths) was measured from the aqueous phase and the values were converted to H2 ssDNA concentration (affinity dissociated) and plotted against initial ssDNA concentrations added. The data points were fitted using non-linear regression analysis and calculated the dissociation constant with the help of SigmaPlot v12 program using one-site saturation, under ligand binding mode which utilized following equation (1)

$$y = B_{max} \bullet \text{free ssDNA}/K_d + \text{free ssDNA} \quad (1)$$

where y is degree of saturation, B_{max} is the number of maximum binding sites (here one-site binding option was employed), K_d is the dissociation constant.[36]

3. Results and discussion

3.1. In vitro selection of anti-HER2 aptamers

Anti-HER2 aptamers were selected in vitro through directed selection by combinatorial screening of random library ~10^{15} ssDNA using SELEX technique. As a result, seven aptamer candidates were evolved that bind to HER2 protein in a complex human serum medium. Sequences of the seven selected aptamers (H1~H7) are listed in Table S1. Binding preference of an aptamer is important for its application as a targeting ligand. An ideal tumor-targeting aptamer should bind to the target molecule with minimal binding to other proteins. Here, we found that H2 sequence evolved multiple times within the window of <50~60 nucleotides from the SELEX process compared with the other aptamer candidates, indicating its strong preference toward binding to HER2 protein. Since albumin is the most abundant protein in blood, we spiked HER2 protein in 1:10 diluted human serum as a background component for in vitro selection and binding studies. The anti-HER2 aptamer (H2) chosen in this study also had a most stable confirmation due to its double strandedness because of its more negative ΔG value after H1 from among the seven aptamer candidates.[34] The calculated ΔG with a following H2 sequence 5'-GGGCCGTCGAACACGAGCATG***GTGCGTGGA***CCTAGGATGACCTGAGTACTGTCC-3' (M.W. = 16.72 kDa) was –6.69 kcal/mole. This result indicated the single strandedness of the aptamer was able to spontaneously transform into its most stable double stranded structure (Fig. 1). The predicted secondary structure of H2 showed two stem-loops and the random sequence was found located in its major stem-loop structure which is predicted to be the binding site for HER2 protein (Fig. 1).

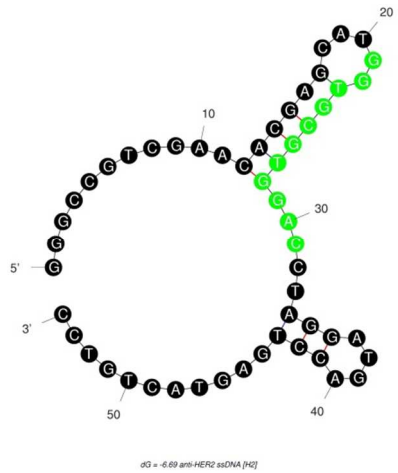

Fig. 1. Secondary structure of anti-HER2 (H2) aptamer predicted using a free energy minimizing algorithm, m-fold web server. The highlighted random region is predicted to be the HER2 protein binding sequence.

3.2. In-vitro affinity dissociation of anti-HER2 aptamers

A new assay scheme was designed for testing in vitro HER2 induced displacement or delivary of anti-HER2 aptamer (H2) to determine their stoichiometric binding or release with respect to H2-to-HER2 protein ratio. Interaction of DNA and CNTs facilitate formation of supramolecular complexes[37] and such interactions have been shown to adhere tightly and form uniform and stable film that has been exploited for useful applications.[38] Here, CNTs were employed as cargos (matrix) for carrying H2 ssDNAs that were coated on MBs to form heterostructures for testing HER2 target protein induced displacement (affinity dissociation) in the medium (Scheme 1).

Analyst RSCPublishing

ARTICLE

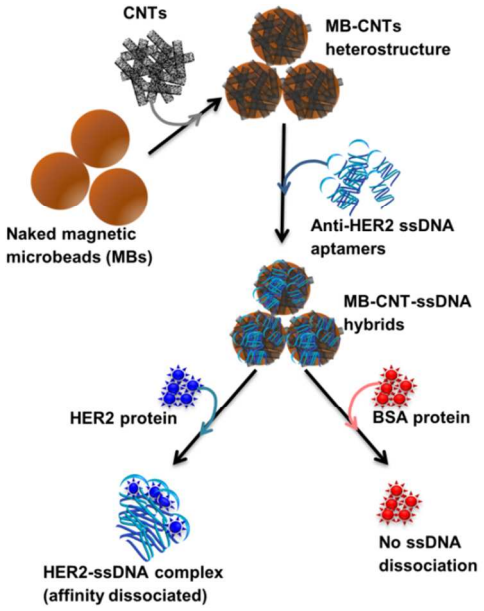

Scheme 1. Schematic diagram showing sequential steps involved in in vitro method employed for HER2 specific targeted release/dissociation of H2 from MB-CNT-H2 cargos. It is to be noted that the graphics of beads, ssDNA or proteins shown in the scheme do not reflect their actual sizes or dimensions.

A heterogenous matrix made of CNTs decorated on MBs were confirmed by SEM examination. Fig. 2a-b shows SEM images of MBs before and after uniform layer coating with CNTs. A small increase in the size of dynabeads was observed after coating with CNTs as seen in Fig. 2b. The H2 ssDNAs were then allowed to tightly pack by physical wrapping on CNTs as described in the experimental section. Binding of fluorescein labelled H2 on MB-CNTs was examined by measuring the fluorescence intensity at 523 nm that showed diminishing fluorescence in the reaction supernatant as a result of strong H2-CNTs interactions compared with the control. The diminishing of fluorescence can be attributed to strong physical wrapping of ssDNAs on CNTs present on MBs. Further, wrapping of ssDNAs on CNT structures was confirmed by FTIR spectra (Fig. S2) The extent of H2 adsorption or loading capacity with 2.8×10^8 MB-CNTs was determined to be in the range 0.025 to 3.125 µM H2 till reaching to a saturation point (Fig. 2c-f).

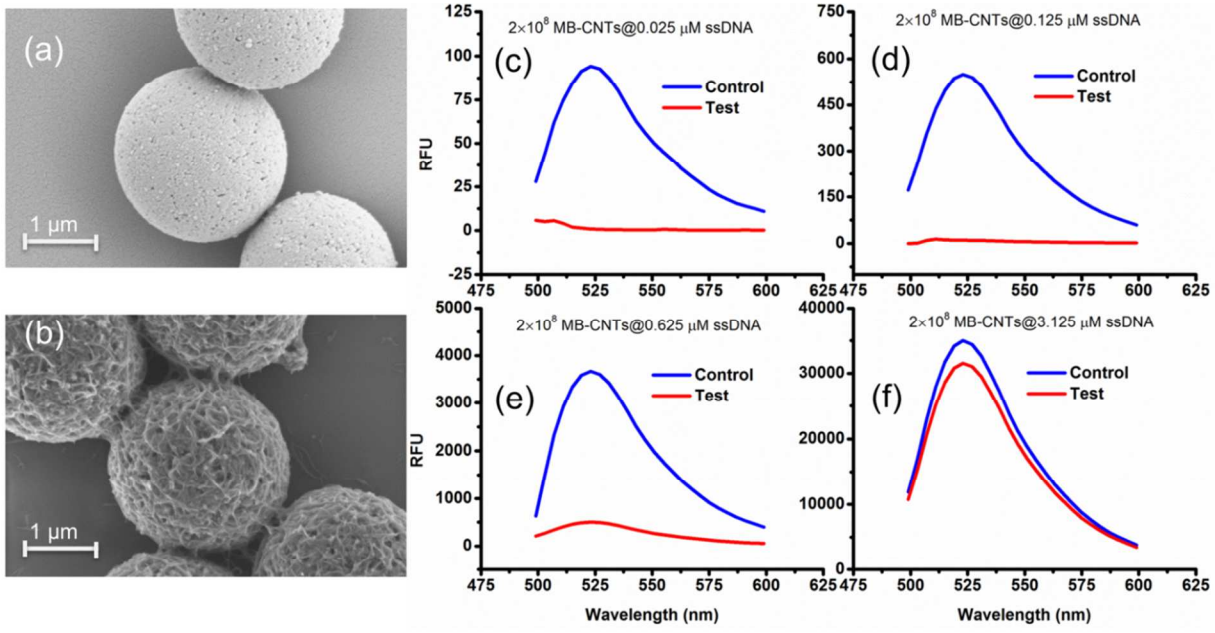

Fig. 2. SEM images of (a) bare MBs and (b) fabricated MB-CNT heterostructures. The MB-CNTs (2×10^8) were loaded with fluorescein labelled H2 ssDNA at different concentrations, such as (c) 0.025 µM, (d) 0.125 µM, (e) 0.625 µM and (f) 3.125 µM and the released fluorescence (after excitation at 470 nm) in the reaction supernatant before (blue) and after incubation (red) with MB-CNTs are shown in the figures (c) to (f) .

3.3. Stability of MB-CNT-H2 hybrid structurers

MB-CNT-H2 hybrid structures were subjected to stability tests by thermal and chemical denaturation. The released fluorescence intensities at 523 nm was measured for the dissocation of CNT wrapped ssDNAs at varying temperatures from 4-94 °C for 1 h. Fluoresence emission profiles of H2 released from MB-CNT-ssDNA hybrids against varying temperatures with time showed no significant unwrapping of ssDNAs occured from CNT-ssDNAs hybrid structures at temperatures 4-94 °C (SI, Fig. 3). However, a partial dissociation of ssDNAs from hybrid structures did occur but only with 0.1% SDS probably due to surfactant-induced unfolding or unwrapping of ssDNAs. It is clear from the above results that the ssDNAs were tightly wrapped on MB-CNTs which required strong surfactive agent like SDS to dissociate from CNTs.

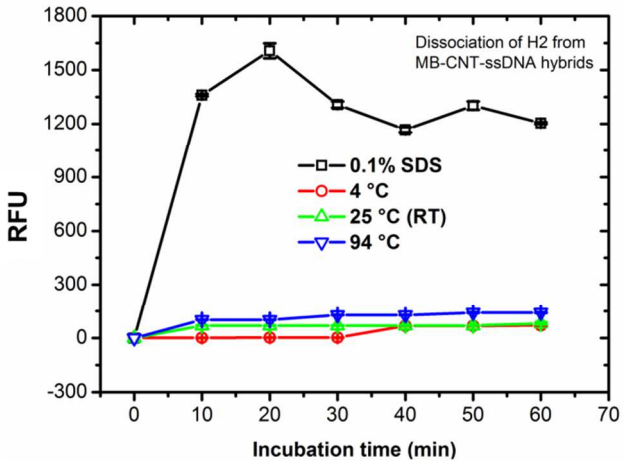

Fig. 3. Stability of MB-CNT-H2 hybrid structure suspending in binding buffer (BB) after thermal and surfactant treatments. Relative fluorescence units (RFU) measured after the MB-CNT-ssDNAs suspension incubated for 1 h at different temperatures or a surfactant as shown in the legend. The figure shows non-specific dissociation of H2 in the aqueous phase of the reaction mixture occured only with the 0.1% SDS.

3.4. In vitro HER2 protein induced affinity release of H2 from MB-CNT-H2 (cargos)

Competitive stoichiometric dissociation of H2 ssDNAs was initially postulated to occur by the influence of HER2 protein in the reaction mixture as schematically illustrated in Scheme 1. This hypothesis was tested by allowing interaction of HER2 protein with MB-CNT-ssDNA hybrid structures (cargos). Dissociation because of the strong binding affinity of H2 toward HER2 protein was therefore determined using a series of MB-CNT-ssDNA hybrid structures ($1\sim5\times10^7$) loaded with 0.05~0.3 µM H2 ssDNAs. These hybrid structures incubated with a constant 300 nM pure and carrier-free form of HER2 protein. HER2 protein induced dissociation of H2 was evidenced from MB-CNT-ssDNA hybrids, which was dose-dependent that accompanied with increase in fluorescence intensity (Fig. 4). The reaction supernatant contained the H2 ssDNA-HER2 protein complex that exhibited fluorescence property because of the fluorescein dye at its 5'-end that did not quench as opposed to that seen with QD-conjugated H2 in dot-blot assays. As the number of MB-CNT-ssDNA conjugates increased, H2 binding with HER2 increased as well until reaching to a saturation point (Fig. 4).

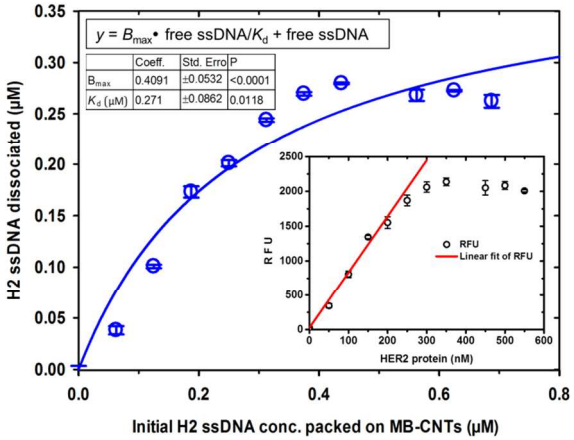

Fig. 4. Binding of HER2 protein with increasing concentrations of free ssDNA (H2) aptamers that were affinity dissociated from the tightly packed MB-CNT-ssDNA hybrid structures. Saturation curve was obtained after plotting the concentration of affinity-dissociated H2 ssDNA against constant HER2 protein (300 nM). The inset figure shows a linear fit of measured RFU values corresponding to the linear range of HER2 protein concentrations.

The H2 ssDNA corresponding to the RFU values were fitted using non-linear regression analysis and the dissociation constant (K_d) according to one-site binding was calculated to be 270 nM with 300 nM HER2 protein present in the reaction mixture. This result indicated approximately, 1:1 stoichiometric molecular binding occurred with ssDNA-to-HER2 protein. Similar 1:1 stoichiometric binding with EGF and EGFR was reported by other research group.[39] Further, a dynamic detection range of 50-250 nM was established using the measured RFU values corresponding to HER2 protein that exhibited a limit of detection of 38 nM (47.5 ng/10 µL sample volume) of HER2 protein (Fig. 4). This range is comparable to previously reported studies.[40]

The specific ability of H2 binding with HER2 protein was confirmed by specificity tests using constant number of MB-CNT-ssDNAs incubated against each protein (HER2/BSA) at equimolar concentrations that showed no non-specific displacement of H2 occurred against BSA protein (Fig. 5). The methods employed in this study, therefore holds an advantage of H2 ssDNA binding with HER2 protein in its native and free forms, which is most desirable in clinical diagnosis and thus making the developed assay, a simple and rapid tool for specific and accurate biomarker detection.

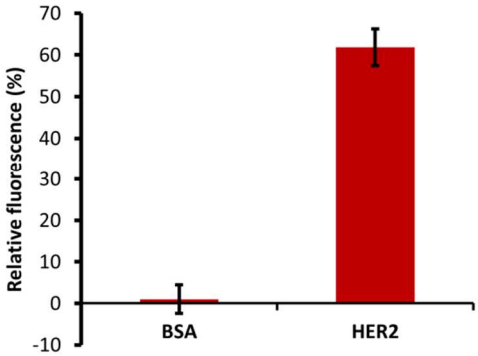

Fig. 5. Affinity dissociation of H2 from a constant MB-CNT-H2 hybrid structures incubated with same amount of BSA and HER2 proteins (300 nM). The H2 aptamer was dissociated only in presence of HER2 protein but not in presence of BSA, a non-specific protein.

Conclusions

Present study provides a unique strategy to target HER2 protein for detection of protein biomarkers in the context of cancer diagnosis or therapy using anti-HER2 aptamers. HER2 is overexpressed in many tumors providing binding sites that can be directly accessible to aptamers from circulating blood. The high affinity and specificity of aptamers with HER2 protein from tumor cells are the useful targets in the sensitive and accurate diagnosis of various types of cancer diseases. In this study, H2 anti-HER2 aptamer was selected in vitro and employed on the basis of its ability to effectively binding to HER2 protein in complex human serum environment. This method did not require any additional chemical reagents enabling detection of HER2 protein in its native forms in human serum making it a most preferred method in clinical diagnosis.

Use of CNTs for targeted delivery is a significant development in the field of therapeutic nanomedicine or diagnosis of cancer where targeting cells that abundantly expressed HER2 protein. The strategy of target induced affinity dissociation is a promising alternative to the existing technologies for cancer diagnosis or therapy. Therefore, a unique in vitro method was developed aiming to test MB-CNTs as cargos of H2 ssDNAs. These cargos were loaded with calculated amounts of fluorescently labelled anti-HER2 aptamer (H2) and successfully tested for its ability to programmable release which was influenced by the presence of abundant HER2 protein in the medium. This strategy can potentially be explored in in vivo models for anti-HER2 aptamers as inhibitory drug-delivery systems. Our study demonstrated that the aptamer mediated cancer diagnosis could be explored further as anti-HER2 therapy or detection of HER2 levels in serum.

Acknowledgements

This work was supported by the Scientific and Technological Research Council of Turkey (TUBITAK), Grant No. 110E287 for JHN. We thank Ashish Pandey, Irena Roci and Lisa Elif Archibald for their assistance with SEM analysis, aptamer selection and binding assays, respectively.

Notes and references

[a] Sabanci University Nanotechnology Research and Application Center, Orta Mah. 34956 Istanbul, Turkey.

[*] Corresponding author E-mail: javed@sabanciuniv.edu; Fax: 90 216 483 9885; Tel: 90 216 483 9879

[b] Department of Pharmaceutical Chemistry, JSS College of Pharmacy, SS Nagara 570015, Mysore, Karnataka, India.

† Electronic Supplementary Information (ESI) available: [Fig. S1 illustrating the SELEX process, FTIR spectra of MB-CNTs and MB-CNTs-ssDNAs (Fig. S2), and the list of aptamer variants (sequences) evolved to bind against HER2 protein after the SELEX process]. See DOI: 10.1039/b000000x/

1. Y. Fukumori and H. Ichikawa, *Advanced powder technology*, 2006, **17**, 1-28.
2. J. K. Vasir and V. Labhasetwar, *Advanced drug delivery reviews*, 2007, **59**, 718-728.
3. A. H. Faraji and P. Wipf, *Bioorganic & medicinal chemistry*, 2009, **17**, 2950-2962.
4. M. Prato, K. Kostarelos and A. Bianco, *Accounts of chemical research*, 2007, **41**, 60-68.
5. S. R. Mane, V. Rao N, K. Chaterjee, H. Dinda, S. Nag, A. Kishore, J. Das Sarma and R. Shunmugam, *Macromolecules*, 2012, **45**, 8037-8042.
6. H. Zhou, W. Yu, X. Guo, X. Liu, N. Li, Y. Zhang and X. Ma, *Biomacromolecules*, 2010, **11**, 3480-3486.
7. A. G. Tkachenko, H. Xie, D. Coleman, W. Glomm, J. Ryan, M. F. Anderson, S. Franzen and D. L. Feldheim, *Journal of the American Chemical Society*, 2003, **125**, 4700-4701.
8. J. Song, J. Zhou and H. Duan, *Journal of the American Chemical Society*, 2012, **134**, 13458-13469.
9. C. Wang, C. Wu, X. Zhou, T. Han, X. Xin, J. Wu, J. Zhang and S. Guo, *Scientific reports*, 2013, **3**.
10. S.-r. Ji, C. Liu, B. Zhang, F. Yang, J. Xu, J. Long, C. Jin, D.-l. Fu, Q.-x. Ni and X.-j. Yu, *Biochimica et Biophysica Acta (BBA)-Reviews on Cancer*, 2010, **1806**, 29-35.
11. R. P. Feazell, N. Nakayama-Ratchford, H. Dai and S. J. Lippard, *Journal of the American Chemical Society*, 2007, **129**, 8438-8439.
12. D. Pantarotto, J.-P. Briand, M. Prato and A. Bianco, *Chemical Communications*, 2004, 16-17.
13. N. W. S. Kam and H. Dai, *Journal of the American Chemical Society*, 2005, **127**, 6021-6026.
14. Y. Liu, D. C. Wu, W. D. Zhang, X. Jiang, C. B. He, T. S. Chung, S. H. Goh and K. W. Leong, *Angewandte Chemie*, 2005, **117**, 4860-4863.
15. N. W. S. Kam, Z. Liu and H. Dai, *Journal of the American Chemical Society*, 2005, **127**, 12492-12493.
16. S. M. Taghdisi, P. Lavaee, M. Ramezani and K. Abnous, *European Journal of Pharmaceutics and Biopharmaceutics*, 2011, **77**, 200-206.
17. N. W. S. Kam, Z. Liu and H. Dai, *Angewandte Chemie*, 2006, **118**, 591-595.
18. R. Stoltenburg, C. Reinemann and B. Strehlitz, *Biomolecular engineering*, 2007, **24**, 381-403.
19. E. M. Reyes-Reyes, Y. Teng and P. J. Bates, *Cancer research*, 2010, **70**, 8617-8629.
20. K.-T. Guo, G. Ziemer, A. Paul and H. P. Wendel, *International journal of molecular sciences*, 2008, **9**, 668-678.
21. E. W. Ng, D. T. Shima, P. Calias, E. T. Cunningham, Jr., D. R. Guyer and A. P. Adamis, *Nature reviews. Drug discovery*, 2006, **5**, 123-132.
22. D. J. Slamon, W. Godolphin, L. A. Jones, J. A. Holt, S. G. Wong, D. E. Keith, W. J. Levin, S. G. Stuart, J. Udove and A. Ullrich, *Science*, 1989, **244**, 707-712.
23. M.-C. Hung, A. Matin, Y. Zhang, X. Xing, F. Sorgi, L. Huang and D. Yu, *Gene*, 1995, **159**, 65-71.
24. M. Milburn, M. Rosman, W. C. Mylander, W. Liang, J. Hooke and A. Kovatich, *Ann Surg Oncol*, 2011, **18**, S176-S176.
25. M. Arnedos, A. Nerurkar, P. Osin, R. A'Hern, I. E. Smith and M. Dowsett, *Ann Oncol*, 2009, **20**, 1948-1952.
26. F. Ciardiello and G. Tortora, *New England Journal of Medicine*, 2008, **358**, 1160-1174.
27. G. Mahlknecht, R. Maron, M. Mancini, B. Schechter, M. Sela and Y. Yarden, *Proceedings of the National Academy of Sciences*, 2013, **110**, 8170-8175.
28. G. C. Shao, J. Wang, Z. H. Li, L. Saraf, W. J. Wang and Y. H. Lin, *Sensor Actuat B-Chem*, 2011, **159**, 44-50.
29. K. Dastjerdi, G. H. Tabar, H. Dehghani and A. Haghparast, *Biotechnology and applied biochemistry*, 2011, **58**, 226-230.
30. C. L. Esposito, D. Passaro, I. Longobardo, G. Condorelli, P. Marotta, A. Affuso, V. de Franciscis and L. Cerchia, *PloS one*, 2011, **6**, e24071.
31. M. Y. Kim and S. Jeong, *Nucleic acid therapeutics*, 2011, **21**, 173-178.
32. B. C. Chi-hong, G. A. Chernis, V. Q. Hoang and R. Landgraf, *Proceedings of the National Academy of Sciences*, 2003, **100**, 9226-9231.
33. R. Stoltenburg, C. Reinemann and B. Strehlitz, *Anal Bioanal Chem*, 2005, **383**, 83-91.
34. M. Zuker, *Nucleic Acids Research*, 2003, **31**, 3406-3415.
35. H. Ünal and J. H. Niazi, *J. Mater. Chem. B*, 2013, **1**, 1894-1902.
36. M. Müller, J. E. Weigand, O. Weichenrieder and B. Suess, *Nucleic acids research*, 2006, **34**, 2607-2617.
37. M. Zheng, A. Jagota, E. D. Semke, B. A. Diner, R. S. Mclean, S. R. Lustig, R. E. Richardson and N. G. Tassi, *Nat Mater*, 2003, **2**, 338-342.
38. C. G. Hu, Y. Y. Zhang, G. Bao, Y. L. Zhang, M. L. Liu and Z. L. Wang, *J Phys Chem B*, 2005, **109**, 20072-20076.
39. P. J. Brennan, T. Kumogai, A. Berezov, R. Murali and M. I. Greene, *Oncogene*, 2000, **19**.
40. J. T. Gohring, P. S. Dale and X. D. Fan, *Sensor Actuat B-Chem*, 2010, **146**, 226-230.

